separations

MDPI

Article

Isolation of (+)-Catechin from Food Waste Using Ionic Liquid-Modified ZIF67 Covered Silica

Mengshuai Liu [1], Xiaoman Li [2], Mengmeng Zhao [1], Xuyang Jiu [1], Chuang Yao [3] and Minglei Tian [1,*]

[1] College of Chemistry and Environmental Engineering, Yangtze University, Jingzhou 434000, China
[2] Changling Branch of Sinopec Catalyst Co., Ltd., Yueyang 414000, China
[3] Guangdong Research Institute of Engineering Technology Co., Ltd., Guangzhou 510000, China
* Correspondence: tianm086@126.com

Abstract

Background: Food waste contains abundant (+)-catechin, but its efficient recovery remains challenging. This study aimed to prepare ionic liquid (IL)-modified sorbents and establish an efficient method for (+)-catechin recovery from chocolate waste via solid-phase extraction (SPE). Methods: Three series of IL-modified sorbents (Sil-IL, ZIF67-IL, Sil@ZIF67-IL) were synthesized. Their adsorption performance was evaluated under different conditions; adsorption isotherm and kinetic data were fitted to Langmuir/Freundlich and pseudo-first/second-order models, respectively. Sorbent stability and (+)-catechin recovery from chocolate waste extracts were tested. Results: Sil@ZIF67-Hmim showed the highest adsorption capacity (154.4 mg/g) at 25 °C within 120 min. Adsorption followed the Langmuir model (R^2 = 0.99), indicating chemisorption. Sil@ZIF67-Hmim was subjected to repeated solid-phase extraction (SPE) for five consecutive days; the recovery rate ranged from 98.1% to 99.2%, and the relative standard deviation (RSD) was 3.2–4.4%. Conclusions: Sil@ZIF67-Hmim is a high-efficiency sorbent for (+)-catechin recovery from chocolate waste, providing a novel approach for food waste valorization and highlighting the application potential of IL-modified MOF-silica composites.

Keywords: ionic liquid; ZIF67; (+)-catechin; chocolate waste; composite silica

1. Introduction

With the continuous growth of the global population, industrial-scale food production has increased significantly. However, due to multiple factors, a substantial amount of food is discarded as waste, resulting in the annual generation of approximately 1.3 billion tons of organic waste—a problem primarily attributed to inadequate storage, expiration, microbial spoilage, physical damage, and other forms of degradation [1]. Despite this, food waste still contains abundant organic components—especially bioactive compounds—that cannot be effectively utilized when food waste is landfilled, incinerated, or processed into animal feed [2]. Numerous studies have shown that bioactive substances such as polyphenols, flavonoids, hydrocarbons, and pigments can be efficiently recovered from food waste via appropriate treatment [3–5].

Flavonoids are naturally occurring bioactive compounds renowned for their antioxidant activity, potential anticancer properties, beneficial effects on metabolic regulation, and protective roles in cardiovascular and cerebrovascular health [6]. (+)-Catechin is a typical flavonoid present in various foods, including grapes, chocolate, and tea. Putra et al. and Tang et al. have reported studies on recovering catechins from peanut skin

Academic Editor: Mingheng Li

Received: 9 January 2026
Revised: 4 February 2026
Accepted: 15 February 2026
Published: 19 February 2026

and grape waste, respectively [7,8]. Thus, the recovery of (+)-catechin from food waste emerges as a promising and sustainable strategy for food waste valorization. Currently, solvent extraction, microwave-assisted extraction, and combined extraction techniques are frequently used to extract (+)-catechin from different sources. For isolation and purification, adsorption-based methods using materials such as resins or molecularly imprinted polymers (MIPs) are considered the most efficient approaches, owing to their high selectivity and adsorption capacity.

The core of adsorption-based methods lies in the development of functional sorbents. Toward this goal, our research group has previously fabricated a series of modified silica sorbents for isolating bioactive compounds from natural plants, where ionic liquids (ILs) played a key role in enhancing adsorption performance. ILs are well recognized as "green" reaction media with excellent chemical properties; their tunable hydrophobicity, miscibility with various inorganic/organic solvents, and specific interactions between functional groups enable their widespread application as solvents or sorbent modifiers [9]. Several studies have demonstrated that IL-modified materials can be used for the extraction and recovery of catechins. For instance, ILs have been applied to extract flavonoids or catechins from grape seeds and tea [10,11], while IL-modified magnetic nanoparticles, silica, and resins have been successfully used to adsorb catechins from grape juice and green tea, respectively [12–14].

These findings indicate that interactions exist between IL groups and catechin molecules, highlighting the potential of IL-modified sorbents for the adsorption and separation of (+)-catechin from complex matrices.

To improve the adsorption selectivity and capacity of sorbents for (+)-catechin, the physicochemical properties of the substrate (in addition to the selection of suitable ILs) exert a critical influence on adsorption efficiency. According to previous studies, metal–organic frameworks (MOFs)—with their unique nanoporous coordination structures—facilitate specific intermolecular interactions [15–17]. ZIF67 is composed of metal ions (Co^{2+}) and the organic compound 2-methylimidazole Co^{2+} coordination clusters and organic ligands jointly construct a three-dimensional porous framework with sodalite topology, and its symmetric cubic lattice structure endows it with high stability [18]. This unique structure endows ZIF67 with a large specific surface area, a uniform microporous structure, and abundant surface active sites [19,20]. These structural features enable ZIF67 to form various intermolecular interactions with (+)-catechin molecules, such as hydrogen bonds, π-π stacking, and coordination interactions, thereby significantly improving its adsorption performance towards (+)-catechin. In this study, ZIF67 was preferentially selected as the adsorbent, primarily due to the fact that the extract of chocolate waste is mostly a neutral/weakly acidic aqueous system. The strong coordination interaction of the zeolitic imidazolate framework in ZIF67 enables the maintenance of structural integrity [21,22]. Studies have demonstrated that ZIF67 holds great application potential in antibiotic wastewater treatment, as its adsorption performance remains stable over a wide pH range [23]. In contrast, the conventional zirconium-based UiO-66 series are mostly synthesized via solvothermal methods [24], whereas ZIF67 can be prepared under room temperature conditions, featuring a straightforward preparation process.

Consequently, IL-modified MOFs have attracted considerable research attention for their tunable separation mechanisms and high enrichment efficiency [25–27]. Yang et al. applied IL-modified MOFs for the adsorption and extraction of bioactive compounds [28], and our team has also established a theoretical foundation for the practical application of IL-modified ZIF67 (a typical MOF) in isolating bioactive compounds from herbal plants [29,30]. However, the stability of IL-modified MOFs in aqueous environments requires further improvement. To overcome this limitation, this study developed an IL-modified ZIF67-

coated silica sorbent and employed a solid-phase extraction (SPE) method for the recovery of (+)-catechin from chocolate waste.

2. Materials and Methods

2.1. Chemicals

Silica (15–31 μm), (3-chloropropyl)trimethoxysilane (98.0%), 2-methylimidazole (98.0%), cobalt nitrate hexahydrate ($Co(NO_3)_2 \cdot 6H_2O$, 99.0%), imidazole (99.0%), N-bromosuccinimide (NBS, 98.0%), 1-chlorobutane (98.0%), 1-chlorohexane (98.0%), and (+)-catechin (97.0%) were purchased from Aladdin Inc. (Shanghai, China). HPLC-grade acetonitrile and methanol were obtained from CINC High Purity Solvents Co., Ltd. (Shanghai, China). Acetonitrile, triethylamine, acetic acid, and other organic solvents were supplied by Beilian Company (Tianjin, China), with purities $\geq$ 99.0%. Ultrapure water was produced using a water purification system (UPH-I-5, Youpu, Mianyang, China).

2.2. Apparatus

Scanning electron microscopy (SEM) images were acquired using a MIRA3 scanning microscope (TESCAN, Brno, Czech Republic). Fourier transform infrared (FT-IR) spectroscopy (Nicolet 6700, Thermo Fisher, Waltham, MA, USA) was performed using KBr pellets over the wavenumber range of 400.0–4000.0 cm^{-1} at a scan rate of 20 scans/min. Thermogravimetric analysis (TGA) was conducted using a Labsys evo instrument (Setaram, Caluire-et-Cuire, France) at a heating rate of 10 °C/min under a nitrogen atmosphere. The BET surface area was measured by ASAP 2460 in N_2 atmosphere (Mi-cromeritics, Norcross, Norcross, GA, USA). HPLC analysis was performed on an LC3000 system (CXTH, Beijing, China) equipped with a TC-C18 column (4.6 × 150.0 mm, 5.0 μm, Agilent, Santa Clara, CA, USA). The mobile phase was acetonitrile/water (20:80, *v*/*v*) containing 1.0% (*v*/*v*) acetic acid, with a flow rate of 0.6 mL/min at a column temperature of 30 °C. Detection was carried out at a UV wavelength of 280.0 nm, and the injection volume was 10.0 μL.

2.3. Preparation of Ionic Liquid-Modified Sorbents

According to our previous study [31], ILs with 4-carbon (butyl) or 6-carbon (hexyl) alkyl chains exhibit enhanced interactions with (+)-catechin due to well-matched hydrophilic–hydrophobic properties. Based on this finding, nine sorbents were prepared (Figure 1).

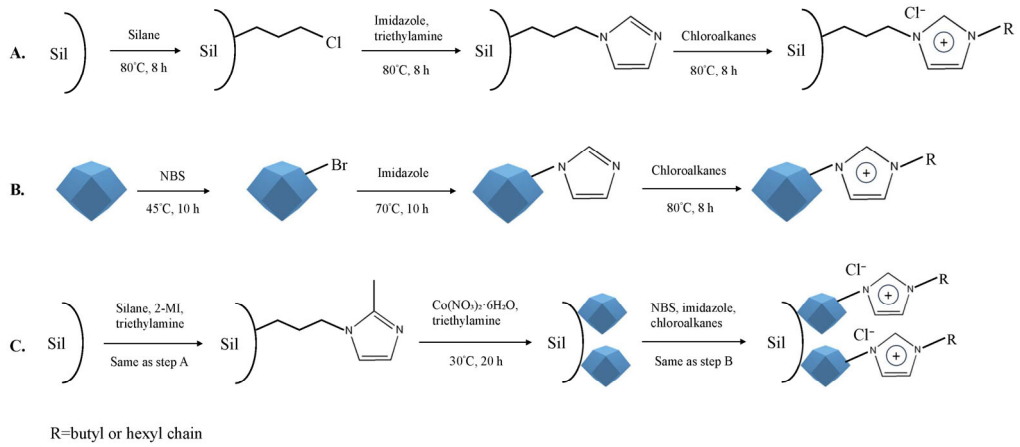

Figure 1. Schematic illustration of the preparation process for ionic liquid (IL)-modified sorbents. (**A**) Synthesis of IL-functionalized silica (Sil) sorbents; (**B**) Synthesis of IL- functionalized ZIF67 sorbents; (**C**) Synthesis of IL- functionalized ZIF67-coated silica (Sil@ZIF67) sorbents.

2.3.1. Step A: Preparation of IL-Modified Silica Sorbents

First, silica was stirred in a 10.0% (v/v) hydrochloric acid aqueous solution for 24 h to activate surface -OH groups. After washing with ultrapure water until the pH reached 7.0, activated silica (Sil) was obtained.

In a round-bottom flask, 20.0 g of Sil and 45.0 g of (3-chloropropyl)trimethoxysilane were mixed with 150.0 mL of toluene. The mixture was heated to 80 °C and stirred for 8 h to synthesize 3-chloropropyl-functionalized Sil. Subsequently, 30.0 g of imidazole, 0.03 g of triethylamine, and 150.0 mL of toluene were added to the flask, and the mixture was stirred at 80 °C for 8 h to produce imidazole-immobilized Sil (Sil-imidazole).

To introduce alkyl chains, 20.0 g of Sil-imidazole was mixed with 150.0 mL of toluene, and 20.0 g of either 1-chlorobutane or 1-chlorohexane was added. The mixture was heated to 80 °C for 8 h, yielding two IL-modified silica sorbents: Sil-Bmim (butyl-modified) and Sil-Hmim (hexyl-modified).

2.3.2. Step B: Preparation of IL-Modified ZIF67 Sorbents

ZIF67 was first synthesized as follows: 15.0 g of $Co(NO_3)_2 \cdot 6H_2O$ and 65.0 g of 2-methylimidazole were separately dissolved in 100.0 mL of methanol under ultrasonic irradiation. The 2-methylimidazole solution was then slowly added dropwise to the stirred $Co(NO_3)_2$ solution. The mixture was stirred continuously at 25 °C for 8 h and aged at room temperature for 16 h. The resulting precipitate was collected by centrifugation at 5000 rpm for 5 min, washed three times with methanol, and dried in an oven at 70 °C for 10 h to obtain purple ZIF67 powder. Next, 4.5 g of ZIF67 and 4.2 g of NBS were mixed in 80 mL of dichloromethane under ultrasonic irradiation. The mixture was heated to 45 °C stirred and reacted for 10 h. The solid product (ZIF67-Br) was collected by centrifugation (5000 rpm, 5 min), washed five times with dichloromethane, and dried at 50 °C for 10 h. Then, 4.0 g of ZIF67-Br, 2.0 g of triethylamine, and 11.5 g of imidazole were added to 150 mL of ethanol in a flask. The mixture was heated to 70 °C and reacted for 10 h; after washing and drying (same as above), imidazole-immobilized ZIF67 (ZIF67-Imidazole) was obtained. Finally, 4.0 g of ZIF67 was mixed with 100.0 mL of ethanol, followed by the addition of 10.0 g of 1-chlorobutane. The mixture was heated to 80 °C and stirred, and reacted for 8 h to afford ZIF67-Bmim. Separately, 4.0 g of ZIF67 was dispersed in 100.0 mL of ethanol, and 10.0 g of 1-chlorohexane was introduced into the system. The resultant mixture was heated to 80 °C and stirred for 8 h, yielding ZIF67-Hmim.

2.3.3. Step C: Preparation of IL-Modified ZIF67-Coated Silica Sorbents

Sil was first modified with 2-methylimidazole using the same method as described in Step A (imidazole immobilization). Then, 30.0 g of 2-methylimidazole-modified Sil, 25.8 mL of triethylamine, and 20.0 g of $Co(NO_3)_2 \cdot 6H_2O$ were dissolved in 100.0 mL of ultrapure water. The mixture was stirred continuously and aged at room temperature for 16 h. The precipitate (Sil@ZIF67) was collected by centrifugation (5000 rpm, 5 min), washed three times with methanol, and dried at 60 °C for 12 h. Finally, following the same procedure as outlined in Step B, Sil@ZIF67 was first mixed with NBS in dichloromethane under ultrasonic irradiation, and the mixture was reacted at 45 °C for 10 h to afford Sil@ZIF67-Br. Subsequently, the product obtained from the above step was reacted with imidazole in ethanol at 70 °C for 10 h to yield Sil@ZIF67-imidazole. Ultimately, Sil@ZIF67-imidazole was separately reacted with equimolar 1-chlorobutane and 1-chlorohexane, affording Sil@ZIF67-Bmim and Sil@ZIF67-Hmim, respectively.

2.4. Adsorption Isotherm and Kinetics Studies Experiments

A calibration curve for (+)-catechin was constructed using seven concentrations (0.0001–0.5 mg/mL). The linear regression equation was $y = 0.19x + 0.001$ (where y is peak area and x is (+)-catechin concentration, mg/mL), and the correlation coefficient (R^2) of 0.97, indicating good linearity.

2.4.1. Adsorption Capacity Evaluation

To determine the maximum adsorption capacity of each sorbent, 0.005 g of sorbent was mixed with 4.0 mL of 0.45 mg/mL (+)-catechin aqueous solution and continuously shaken at 25 °C for 10 h. After adsorption equilibrium, the residual (+)-catechin concentration was measured by HPLC.

2.4.2. Adsorption Isotherm Experiments

For isotherm studies, 0.005 g of sorbent was mixed with 4.0 mL of (+)-catechin aqueous solution with concentrations ranging from 0.001 to 0.45 mg/mL at 25 °C. The concentrations of (+)-catechin before and after adsorption were determined by HPLC. The equilibrium adsorption capacity (Q_e, mg/g) and adsorption efficiency (E%) were calculated using Equations (1) and (2):

$$Q_e = \frac{(C_0 - C_e) \times V}{m} \quad (1)$$

$$E\% = \frac{(C_0 - C_e) \times V}{C_0 \times V} \times 100\% \quad (2)$$

where C_0 (mg/mL) is initial (+)-catechin concentration, C_e (mg/mL) is equilibrium (+)-catechin concentration, V (mL) is solution volume, and m (g) is sorbent mass.

2.4.3. Adsorption Kinetics Experiments

For kinetics studies, 0.005 g of sorbent was added to 4.0 mL of 1.0 mg/mL (+)-catechin solution at 30 °C, and samples were collected at different time intervals (1.0–120.0 min). The experimental data were fitted to pseudo-first-order (Equation (3)) and pseudo-second-order (Equation (4)) kinetic models:

$$ln(Q_e - Q_t) = lnQ_e - k_1 t \quad (3)$$

$$\frac{t}{Q_t} = \frac{1}{k_2 Q_e^2} + \frac{t}{Q_e} \quad (4)$$

where Q_t (mg/g) is adsorption capacity at time t (min), k_1 (min^{-1}) is pseudo-first-order rate constant, and k_2 (g/(mg·min)) is pseudo-second-order rate constant.

2.5. Stability and Reusability Tests

To evaluate sorbent reusability, 0.015 g of sorbent was mixed with 1.0 mL of 1.0 mg/mL (+)-catechin aqueous solution at 30 °C for 120.0 min. After measuring the residual (+)-catechin concentration by HPLC, the sorbent was desorbed by eluting and rinsed thoroughly with a methanol/water mixture (70:30, v/v). The adsorption–desorption cycle was repeated under identical conditions for more than 10 cycles, and the adsorption capacity was determined after each cycle.

2.6. Isolation of (+)-Catechin from Chocolate Waste Using SPE

First, (+)-catechin was extracted from chocolate waste: 10.0 g of cocoa shell waste powder (a byproduct of chocolate production) was immersed in 20.0 mL of water at 65 °C and continuously stirred for 8 h. The extract was collected and filtered through a 0.22 µm nylon membrane. For SPE, 0.3 g of sorbent was packed into a standard SPE cartridge

(Φ 0.9 cm) and preconditioned with 6.0 mL of methanol. The filtered cocoa shell extract was then loaded onto the cartridge, and the effluent was collected. To elute (+)-catechin, 3.0 mL portions of eluents with different polarities (water, acetonitrile, methanol, or methanol/water containing 1% (*v*/*v*) acetic acid) were passed through the cartridge at a flow rate of 0.6 mL/min. The eluate was analyzed by HPLC to determine the (+)-catechin recovery rate.

3. Results and Discussion

3.1. Characterization

The SEM microstructures of Sil@ZIF67-IL are illustrated in Figure 2. As depicted in Figure 2D, well-defined rhombic dodecahedral crystals with uniform particle sizes (≈200–300 nm) are distinctly observed, which is consistent with the characteristic morphology of ZIF67, thereby confirming the successful synthesis of the metal-organic framework. In Figure 2B, the crystals exhibit slightly rough surfaces, indicative of the successful grafting of ionic liquid (IL) onto the MOF matrix. Figure 2A presents the silica substrate under low magnification, while Figure 2C reveals numerous dodecahedral particles uniformly dispersed on the silica surface, demonstrating that ZIF67-IL crystals are firmly anchored onto the silica support. This hierarchical architecture is advantageous for exposing active adsorption sites and facilitating mass transfer, thus enhancing the adsorption performance. In summary, the SEM characterization results unequivocally verify the successful fabrication of Sil@ZIF67-IL.

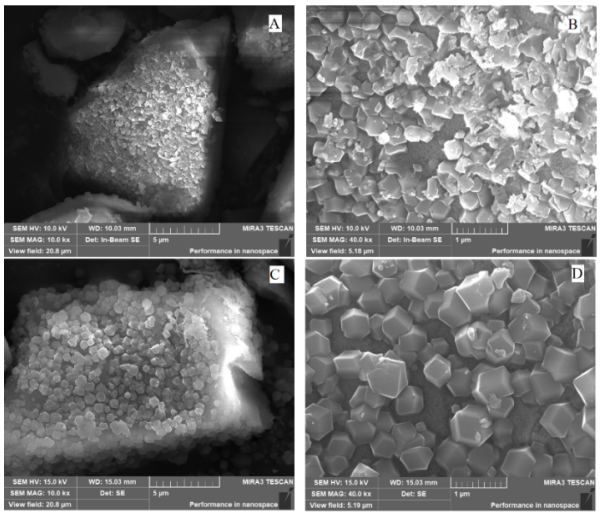

Figure 2. Scanning electron microscopy (SEM) images of Sil (**A**), ZIF67-IL (**B**), and Sil@ZIF67-IL (**C**,**D**) at different magnifications.

The FTIR spectra of the materials are presented in Figure 3. Silica (Sil) shows a prominent absorption peak around 1100 cm^{-1}, which corresponds to the stretching vibration of Si-O-Si bonds. ZIF67-Hmim as ZIF-IL exhibits characteristic peaks in the range of 1400–1600 cm^{-1}, which are attributed to the C=N and C=C skeletal vibrations of the imidazole ring—confirming the intact presence of both ZIF67 and IL structures. For the composite Sil@ZIF67-Hmim, the Si-O characteristic peaks (1000–1200 cm^{-1}) and ZIF67-Hmim characteristic peaks (1400–1600 cm^{-1}) are observed simultaneously. This spectral overlap verifies the successful fabrication of the Sil@ZIF67-Hmim.

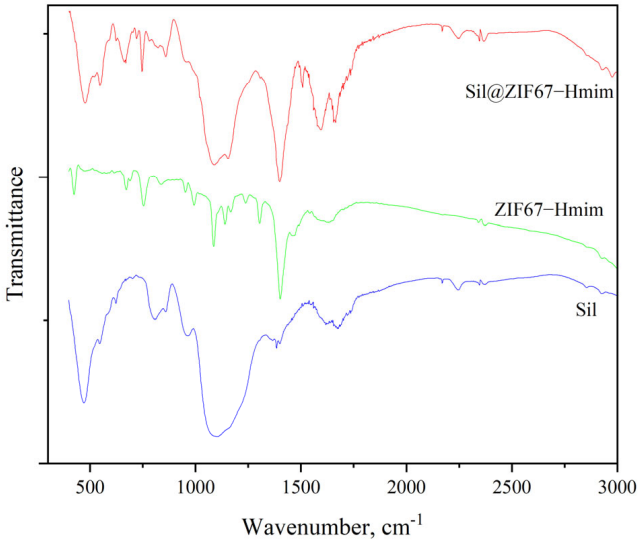

Figure 3. Fourier transform infrared (FTIR) spectra of Sil, ZIF67-Hmim, and Sil@ZIF67-Hmim.

The surface areas of different materials detected via BET can also verify the successful fabrication. The blank silica was 48.3 m^2/g, and after modifying with ZIF-IL, the surface area of Sil@ZIF67-IL exhibited a much larger surface area of 188.8 m^2/g because of the porous structure and nanoscale size of ZIF67-IL.

The thermal decomposition curves of Sil-IL, ZIF67-IL, and Sil@ZIF67-IL were acquired via thermogravimetric analysis (TGA), as depicted in Figure 4. For Sil-IL (Figure 4A), the mass started to decrease above 450 °C with a maximum mass loss of 20.45%, indicating the decomposition of the ionic liquid (IL) grafted on Sil at elevated temperatures. For ZIF-IL (Figure 4B), a slow mass loss was observed before 460 °C, corresponding to the gradual decomposition of organic groups in ZIF67, followed by an abrupt drop, which indicates the co-decomposition of organic groups and IL under high temperatures. As for Sil@ZIF67-IL (Figure 4C), the material first underwent a 41.45% mass loss and subsequently experienced further mass loss, resulting in a total mass loss of 61.74%, demonstrating that ZIF67 and IL moieties modified on the Sil surface decomposed at distinct temperature intervals. These TGA results verify the successful synthesis of the target materials.

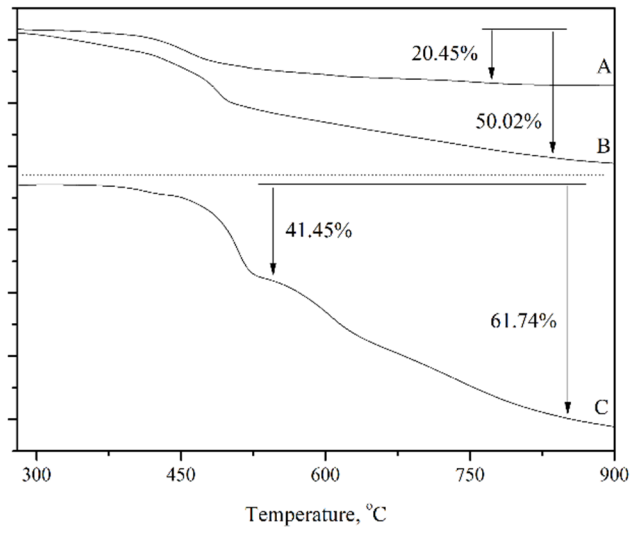

Figure 4. Thermogravimetric analysis (TGA) curves of Sil-IL (**A**), ZIF67-IL (**B**), and Sil@ZIF67-IL (**C**).

3.2. Comparison of Maximum Adsorption Capacity

Figure 5 presents the maximum adsorption capacities of all nine sorbents. The adsorption capacities of ZIF67 and Sil@ZIF67 were significantly higher than those of Sil, which can be attributed to the larger specific surface area of ZIF67 with its nanoporous structure, compared with that of microscale silica. Additionally, Sil-Bmim and Sil-Hmim exhibited a notable increase in adsorption capacity relative to unmodified Sil, confirming the strong interactions between IL groups and (+)-catechin.

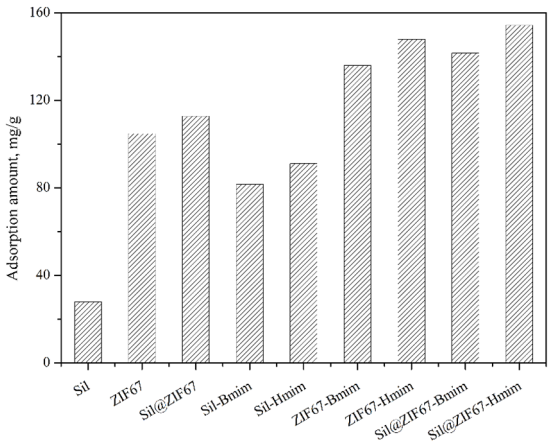

Figure 5. The maximum adsorption capacities of the nine synthesized sorbents.

The composite sorbents (ZIF67-Bmim, ZIF67-Hmim, Sil@ZIF67-Bmim, and Sil@ZIF67-Hmim) achieved the highest adsorption capacities, as they combined two advantages: the large specific surface area of ZIF67 (providing abundant adsorption sites) and the specific interactions between IL groups and (+)-catechin. These results demonstrate that the rational design of composite sorbents—guided by the chemical structure and functional groups of (+)-catechin—effectively improves adsorption efficiency.

3.3. Adsorption Isotherm and Kinetics Studies

3.3.1. Adsorption Isotherm Studies

Figure 6a shows the adsorption isotherms of the six IL-modified sorbents (Sil-Bmim, Sil-Hmim, ZIF67-Bmim, ZIF67-Hmim, Sil@ZIF67-Bmim, and Sil@ZIF67-Hmim). With increasing (+)-catechin concentration, the adsorption capacity of all sorbents increased, which is consistent with the principle of mass transfer driving force: higher initial concentrations promote the diffusion of (+)-catechin molecules toward the sorbent surfaces.

The mechanism underlying the enhanced adsorption of IL-modified sorbents involves three key types of interactions: (1) Hydrogen bonding between the -OH/-O- groups of (+)-catechin and the imidazole groups of ILs; (2) Ionic interactions between the negatively charged phenolic groups of (+)-catechin and the positively charged imidazolium cations of ILs; (3) π-π stacking between the benzene ring of (+)-catechin and the imidazole ring of ILs (enhancing adsorption selectivity).

The Langmuir model (R^2 = 0.99) provided a better fit than the Freundlich model (R^2 = 0.94), indicating that the adsorption of (+)-catechin onto the sorbents follows a monolayer adsorption mechanism—consistent with the uniform distribution of IL groups on the sorbent surface and the specific 1:1 interaction between IL groups and (+)-catechin molecules.

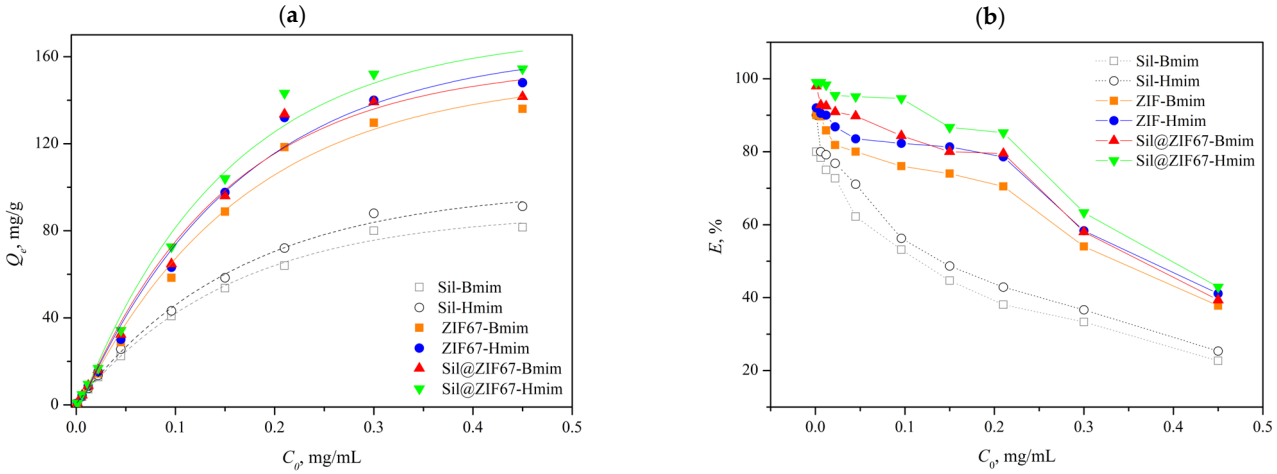

Figure 6. (**a**) Adsorption isotherms and (**b**) adsorption efficiencies (*E*%) of the six IL-modified sorbents.

For Sil-Bmim and Sil-Hmim, the introduction of IL groups improved adsorption capacity, but this effect was offset by the small specific surface area of silica. Additionally, the significant decrease in *E*% with increasing (+)-catechin concentration (Figure 6b) suggests that the long alkyl chains of ILs blocked some surface -OH groups of silica during modification, reducing the number of available adsorption sites for (+)-catechin.

ZIF67-Bmim and ZIF67-Hmim exhibited higher adsorption capacities than Sil-Bmim and Sil-Hmim, owing to the large specific surface area of ZIF67. However, their adsorption capacities were lower than expected, as the dense packing of IL groups on the nanoporous surface caused steric hindrance of ZIF67—preventing some IL groups from interacting with (+)-catechin.

Sil@ZIF67-Bmim and Sil@ZIF67-Hmim achieved the highest adsorption capacities among all sorbents, which can be attributed to two synergistic effects: (1) The ZIF67 coating on silica maintained a large specific surface area (provided by Co^{2+}-coordinated nanopores); (2) The unblocked -OH groups on silica contributed additional adsorption sites via hydrogen bonding with (+)-catechin. When the initial (+)-catechin concentration exceeded 0.3 mg/mL, the adsorption capacity of all sorbents tended to plateau (Figure 6a), and *E*% decreased slightly (Figure 6b). This indicates that the adsorption sites on the sorbents approached saturation. Subsequent studies (including those on temperature effects and adsorption kinetics) were focused on the four composite sorbents (ZIF67-Bmim, ZIF67-Hmim, Sil@ZIF67-Bmim, and Sil@ZIF67-Hmim) due to their higher adsorption capacities.

3.3.2. Effect of Temperature on Adsorption Capacity

Figure 7 shows the effect of temperature (25–55 °C) on the adsorption capacities of the four composite sorbents. With increasing temperature, the adsorption capacity of all sorbents decreased. This phenomenon can be explained by the nature of intermolecular interactions: higher temperatures increase the kinetic energy of (+)-catechin molecules, weakening the hydrogen bonding, ionic interactions, and π-π stacking between (+)-catechin and sorbents [29].

Notably, the adsorption capacities of Sil@ZIF67-Bmim and Sil@ZIF67-Hmim decreased less significantly than those of ZIF67-Bmim and ZIF67-Hmim. This is because the silica substrate improved the thermal stability of the composite sorbents: the -OH groups of silica form stronger hydrogen bonds with (+)-catechin than the IL groups of ZIF67, making them less sensitive to temperature changes. Based on these results, 25 °C was selected as the optimal temperature for subsequent experiments.

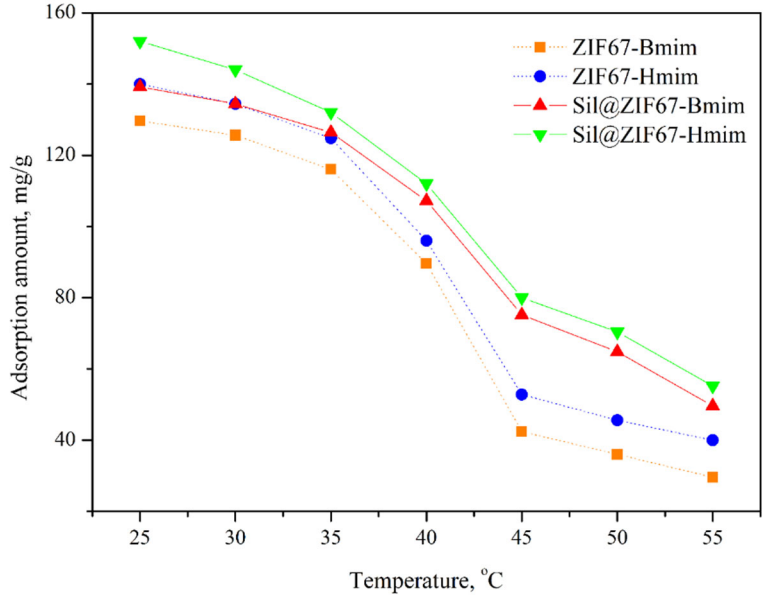

Figure 7. Effect of temperature on the adsorption capacities of the four composite sorbents.

3.3.3. Adsorption Kinetics

Figure 8 shows the adsorption kinetics of the four composite sorbents. The adsorption capacities increased rapidly in the first 30 min (due to the abundance of vacant adsorption sites on sorbent surfaces) and gradually approached equilibrium. Specifically, ZIF67-Bmim and ZIF67-Hmim reached equilibrium at 80 min, while Sil@ZIF67-Bmim and Sil@ZIF67-Hmim required 120 min to reach equilibrium. The longer equilibrium time of Sil@ZIF67-based sorbents was attributed to their thicker ZIF67 coating, which increases the diffusion distance of (+)-catechin molecules into the sorbent interior.

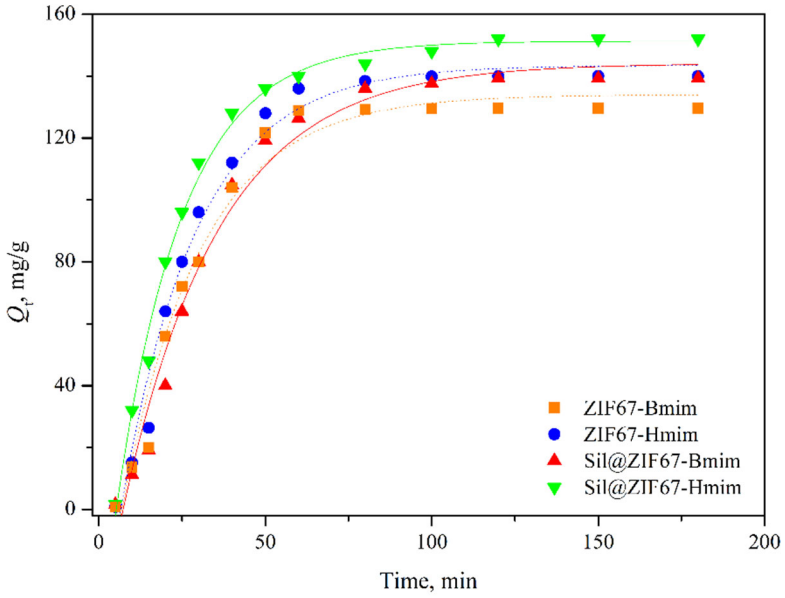

Figure 8. Adsorption kinetics of the four composite sorbents.

The pseudo-second-order model (R^2 = 0.97) provided a much better fit than the pseudo-first-order model (R^2 = 0.84), indicating that the adsorption process is dominated by chemical adsorption (e.g., ionic interactions, hydrogen bonding) rather than physical adsorption (e.g., van der Waals forces) [32]. Based on these results, an adsorption time of 120 min was recommended for subsequent experiments to ensure equilibrium.

3.4. Other Factors Affecting Adsorption Capacity

3.4.1. Effect of Water: Methanol Ratio

Figure 9 shows the effect of water/methanol ratio (0:100–100:0, v/v) on the adsorption capacities of the four composite sorbents. For ZIF67-Bmim and ZIF67-Hmim, the adsorption capacity decreased significantly with increasing water content. This is because water molecules disrupt the coordination bonds between Co^{2+} and imidazole ligands in the ZIF67 components, leading to structural degradation of the sorbents.

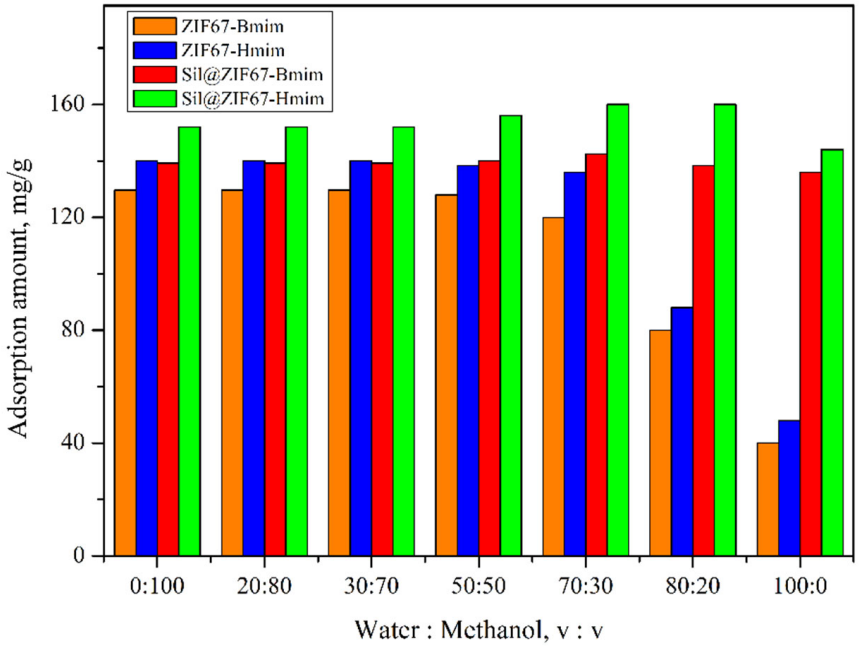

Figure 9. Effect of water/methanol volume ratio on the adsorption capacities of the four composite sorbents (measured at 25 °C, initial (+)-catechin concentration was 0.3 mg/mL, adsorption time was 120 min).

In contrast, the adsorption capacity of Sil@ZIF67-Bmim and Sil@ZIF67-Hmim first increased slightly (water/methanol was 0:100–70:30) and then decreased (water/methanol was 70:30–100:0). The initial increase can be attributed to the hydrophobicity of (+)-catechin: higher water content enhances the hydrophobic interaction between (+)-catechin and the alkyl chains of ILs, promoting adsorption. The subsequent decrease (pure water) is due to the disruption of hydrogen bonding between silica -OH groups and (+)-catechin by an excess of water molecules.

Based on these results, a water/methanol ratio of 70:30 (v/v) was selected as the optimal solvent system. ZIF67-Bmim and ZIF67-Hmim were excluded from further studies due to their poor hydrolytic stability in aqueous solutions.

3.4.2. Effect of Solution pH

The effect of solution pH (3.0–9.0) on the adsorption capacities of Sil@ZIF67-Bmim and Sil@ZIF67-Hmim was investigated under the following conditions: water/methanol ratio of 70:30 (v/v), (+)-catechin concentration of 0.3 mg/mL, contact time of 120 min, and temperature of 25 °C (Figure 10).

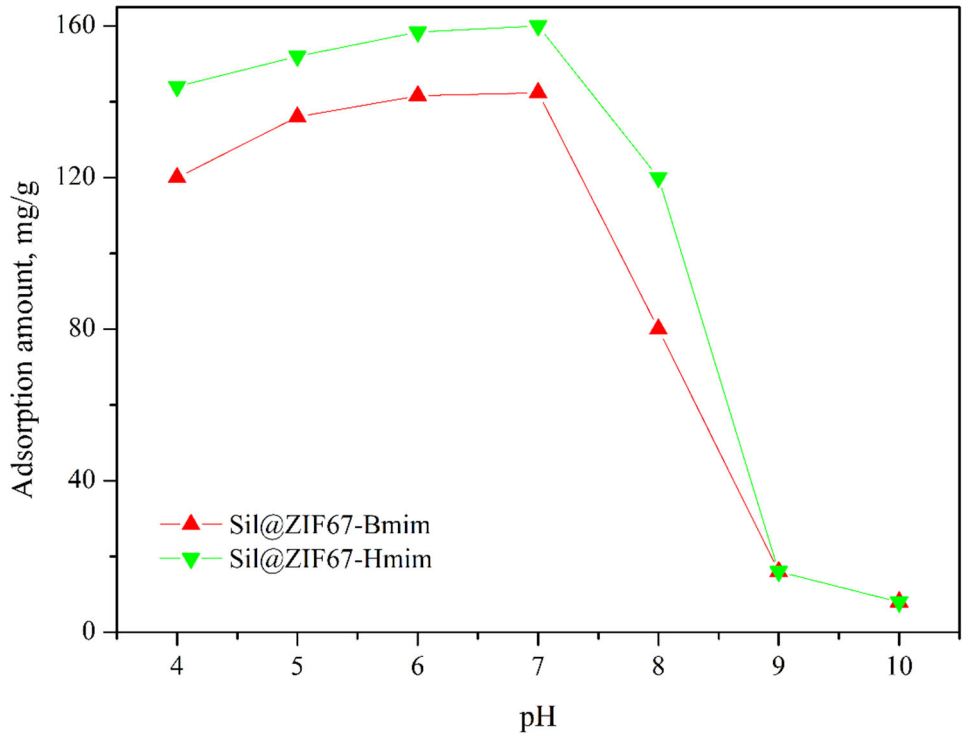

Figure 10. Effect of solution pH on the adsorption capacities of Sil@ZIF67-Bmim and Sil@ZIF67-Hmim (measured at 25 °C, 0.3 mg/mL (+)-catechin, 120 min adsorption time, water/methanol was 70:30 (*v*/*v*)).

When pH < 7.0 (acidic conditions), the adsorption capacity decreased slightly. This is because excess H^+ ions in acidic solutions compete with (+)-catechin for adsorption sites: H^+ binds to the imidazole groups of ILs (protonation) and the -OH groups of silica, weakening hydrogen bonding and ionic interactions with (+)-catechin. Also, the isoelectric point (pHzpc) study of the Sil@ZIF67-IL surface was performed at pH 5.1; therefore, under acidic conditions, the adsorption capacity of (+)-catechin was low because of the repulsion between (+)-catechin and the positively charged Sil@ZIF67-IL surface.

When pH > 7.0 (alkaline conditions), the adsorption capacity decreased significantly. Alkaline environments cause the deprotonation of silica -OH groups (forming SiO^- species) and the hydrolysis of Co^{2+} in ZIF67, leading to structural deterioration of the sorbents.

Thus, a neutral pH of 7.0 was determined to be optimal for the adsorption of (+)-catechin onto Sil@ZIF67-Bmim and Sil@ZIF67-Hmim.

3.5. Stability and Reusability of Sil@ZIF67-Hmim

The adsorption capacities of Sil-Hmim, ZIF67-Hmim, and Sil@ZIF67-Hmim were tested during the repeated adsorption and desorption processes, and after 10 adsorption–desorption cycles, the adsorption capacities decreased by 2.5%, 3.6%, and 0.7%, respectively. The results revealed that the structural stability of Sil@ZIF67-Hmim was more stable than that of other sorbents. The limit of detection (LOD) and limit of quantitation (LOQ) were determined to be 0.003 mg/L and 0.02 mg/L, respectively, demonstrating that the analytical conditions were sufficiently precise.

3.6. Solid-Phase Extraction of (+)-Catechin from Chocolate Waste

First, the extract obtained from chocolate waste was analyzed. HPLC analysis of the injected sample yielded a (+)-catechin concentration of 2.24 mg/g (Figure 11A). Subsequently, 0.05 g of the adsorbent Sil@ZIF67-Hmim was weighed out and packed into a SPE cartridge. The extract was loaded onto the cartridge, and the cartridge was then placed in

an incubator at 30 °C. After incubation for 60 min, the adsorbent was rinsed with hexane to eliminate interference from impurities. Then, methanol was used as the elution solvent to desorb (+)-catechin from the adsorbent. As shown in (Figure 11B), the impurity peaks were basically removed. Finally, the adsorbent was rinsed again with methanol/acetic acid solution. HPLC analysis results (Figure 11C) indicated that (+)-catechin had been completely eluted. The SPE method could separate all (+)-catechin from chocolate waste, and the adsorbent could be used for subsequent adsorption–desorption cycles.

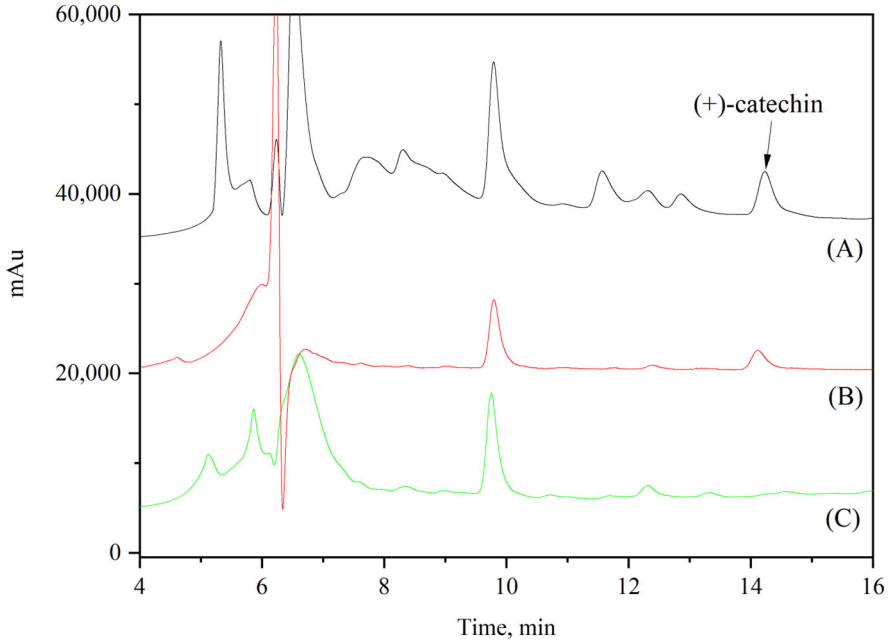

Figure 11. High-performance liquid chromatography (HPLC) chromatograms of different steps in the solid-phase extraction (SPE) process: (**A**) Chocolate waste extract; (**B**) Eluate with methanol; (**C**) Eluate with methanol/acetic acid solution (1%, *v*/*v*).

Then, a 1.0 mg/mL standard solution of (+)-catechin was spiked into the chocolate waste extract; the recoveries of (+)-catechin in the SPE process were calculated using the HPLC peak areas and the correlation equation. Moreover, the relative standard deviations (RSDs) were analyzed by repeating the SPE process five times per day (intra-day RSD) under exactly the same conditions over five consecutive days (inter-day RSD). The satisfactory recoveries of 98.1–99.2% and RSDs of 3.2–4.4% revealed that the SPE method using Sil@ZIF67-Hmim was accurate and precise to isolate (+)-catechin from chocolate waste.

3.7. Comparison with Reported Sorbents for (+)-Catechin Adsorption

After reviewing previous studies, we compared the performance of several different adsorbents for (+)-catechin adsorption (Table 1). Yusoff et al. constructed a core-shell magnetite-hydroxyapatite nanoparticle (Fe_3O_4/HA) catechin delivery system with a maximum loading capacity of 110.97 mg/g [33]. Jabbari et al. successfully prepared UIO66-NH_2@PANI nanocomposites for efficient catechin adsorption, achieving an adsorption capacity of 69.15 mg/g at pH 10 [34]. In a previous study on Sil@ZIF8@EIM-EIM, an adsorbent developed for extracting (+)-catechin from cacao shells, the maximum adsorption capacity was 58.0 mg/g [31]. In contrast, the maximum adsorption capacity in this study was significantly improved. Additionally, some studies have reported other methods for extracting (+)-catechin from plants. Rezaeinejad et al. established a high-efficiency and rapid magnetic solid-phase extraction (MSPE) method based on ionic liquid-modified magnetic nanoparticles, utilizing sample-loaded narrow-bore tubes for (+)-catechin extraction from grape juice, with a maximum adsorption capacity of 61 mg/g [12].

Table 1. Comparison of the methods or proposed material for catechin.

Sorbent	Adsorption Method	Capacity (mg/g)	RSD (%)	Ref.
Fe_3O_4/HA	SPE	110.97 mg/g	-	[33]
UIO66-NH_2@PANI	-	69.15 mg/g	-	[34]
Sil@ZIF8@EIM-EIM	SPE	58.0 mg/g	1.3–3.2%	[31]
Fe_3O_4@IL Nanoparticles	MSPE	61 mg/g	1.63%	[12]
CS-LIG	-	115.67 mg/g	-	[35]
Sil@ZIF67-Hmim	SPE	154.4 mg/g	3.2–4.4%	This work

Zhu, Y. et al. prepared a CS-DES lignin aerogel via solution blending and copper block freeze-drying technology, which exhibited a maximum (+)-catechin adsorption capacity of 115.67 mg/g. After 4 adsorption–desorption cycles, the adsorption capacity decreased by 1.3% [35]. Overall, the adsorbent successfully prepared in this study, which achieved a maximum adsorption capacity of 154.4 mg/g, enables efficient adsorption of (+)-catechin and exhibits superior adsorption performance compared with those of other reported adsorbents.

4. Conclusions

In this study, an ionic liquid-modified ZIF67-coated silica sorbent (Sil@ZIF67-Hmim) was successfully synthesized for the recovery of (+)-catechin from chocolate waste. The interactions between Sil@ZIF67-Hmim and (+)-catechin were primarily evaluated based on static adsorption capacities under various conditions. The composite sorbent exhibited a high maximum adsorption capacity (154.4 mg/g) and excellent selectivity for (+)-catechin, which were attributed to the synergistic effects of the large specific surface area of ZIF67 and the specific interactions (hydrogen bonding, ionic interactions, and π-π stacking) between IL groups and (+)-catechin molecules.

Adsorption isotherm and kinetic studies revealed that the adsorption process followed the Langmuir monolayer model and pseudo-second-order kinetics, confirming chemical adsorption as the dominant mechanism. The sorbent also demonstrated excellent stability and reusability (after 10 adsorption–desorption cycles, the adsorption capacity decreased by 0.7%). After Sil@ZIF67-Hmim was packed into a SPE cartridge, the cartridge successfully separated all (+)-catechin from chocolate waste.

This work provides a novel and efficient approach for the valorization of food waste (via the recovery of bioactive (+)-catechin) and highlights the potential of IL-modified MOF-silica composites for environmental and food chemistry applications.

Author Contributions: M.L. and X.L. conceived the study. M.L. performed the experiments and analyzed the data. M.Z. and X.J. contributed to the material preparation. M.T. and C.Y. designed the study and revised the manuscript. All authors have read and agreed to the published version of the manuscript.

Funding: This research was funded by the National Natural Science Foundation of China (No. 51503020).

Data Availability Statement: Data are contained within the article.

Conflicts of Interest: Author Xiaoman Li was employed by the company Changling Branch of Sinopec Catalyst Co., Ltd., Yueyang 414000, China. The remaining authors declare that the research was conducted in the absence of any commercial or financial relationships that could be construed as a potential conflict of interest. Author Chuang Yao was employed by the company Guangdong Research Institute of Engineering Technology Co., Ltd., Guangzhou 510000, China. The remaining authors declare that the research was conducted in the absence of any commercial or financial relationships that could be construed as a potential conflict of interest.

References

1. Jimenez, M.E.C.; Gabilondo, J.; Bodoira, R.M.; Laverde, L.M.A.; Santagapita, P.R. Extraction of bioactive compounds from pecan nutshell: An added-value and low-cost alternative for an industrial waste. *Food Chem.* **2024**, *453*, 139596. [CrossRef] [PubMed]
2. Pires, E.O.; Caleja, C.; Garcia, C.C.; Ferreira, I.C.; Barros, L. Current status of genus Impatiens: Bioactive compounds and natural pigments with health benefits. *Trends Food Sci. Technol.* **2021**, *117*, 106–124. [CrossRef]
3. de Oliveira, A.; Valentim, I.; Silva, C.A.; Bechara, E.J.H.; de Barros, M.P.; Mano, C.M.; Goulart, M.O.F. Total phenolic content and free radical scavenging activities of methanolic extract powders of tropical fruit residues. *Food Chem.* **2009**, *115*, 469–475. [CrossRef]
4. Hellwig, V.; Gasser, J. Polyphenols from waste streams of food industry: Valorisation of blanch water from marzipan production. *Phytochem. Rev.* **2020**, *19*, 1539–1546. [CrossRef]
5. Medina-Torres, N.; Espinosa-Andrews, H.; Trombotto, S.; Ayora-Talavera, T.; Patrón-Vázquez, J.; González-Flores, T.; Sánchez-Contreras, Á.; Cuevas-Bernardino, J.C.; Pacheco, N. Ultrasound-Assisted Extraction Optimization of Phenolic Compounds from Citrus latifolia Waste for Chitosan Bioactive Nanoparticles Development. *Molecules* **2019**, *24*, 3541. [CrossRef]
6. Ettoumi, F.E.; Zhang, R.; Xu, Y.; Li, L.; Huang, H.; Luo, Z. Synthesis and characterization of fucoidan/chitosan-coated nano-liposomes for enhanced stability and oral bio availability of hydrophilic catechin and hydrophobic juglone. *Food Chem.* **2023**, *423*, 136330. [CrossRef]
7. Putra, N.R.; Rizkiyah, D.N.; Qomariyah, L.; Aziz, A.H.A.; Veza, I.; Yunus, M.A.C. Experimental and modeling for catechin and epicatechin recovery from peanut skin using subcritical ethanol. *J. Food Process Eng.* **2023**, *46*, e14275. [CrossRef]
8. Tang, G.Y.; Zhao, C.N.; Liu, Q.; Feng, X.-L.; Xu, X.-Y.; Cao, S.-Y.; Meng, X.; Li, S.; Gan, R.-Y.; Li, H.-B. Potential of Grape Wastes as a Natural Source of Bioactive Compounds. *Molecules* **2018**, *23*, 2598. [CrossRef] [PubMed]
9. Fang, L.; Tian, M.; Yan, X.; Xiao, W.; Row, K.H. Dual ionic liquid-immobilized silicas for multi-phase extraction of aristolochic acid from plants and herbal medicines. *J. Chromatogr. A* **2019**, *1592*, 31–37. [CrossRef] [PubMed]
10. Ran, L.; Yang, C.; Xu, M.; Yi, Z.; Ren, D.; Yi, L. Enhanced aqueous two-phase extraction of proanthocyanidins from grape seeds by using ionic liquids as adjuvants. *Sep. Purif. Technol.* **2019**, *226*, 154–161. [CrossRef]
11. Bajkacz, S.; Adamek, J.; Sobska, A. Application of Deep Eutectic Solvents and Ionic Liquids in the Extraction of Catechins from Tea. *Molecules* **2020**, *25*, 3216. [CrossRef]
12. Rezaeinejad, S.; Hashemi, P.; Rahimi, A. Narrow-Bore Tube Magnetic Solid-Phase Extraction Method Utilizing Ionic Liquid-Modified Magnetic Nanoparticles for the Preconcentration and Determination of Catechin in Grape Juice. *Food Anal. Methods* **2025**, *18*, 416–427. [CrossRef]
13. Zhang, W.; Feng, X.; Alula, Y.; Yao, S. Bionic multi-tentacled ionic liquid-modified silica gel for adsorption and separation of polyphenols from green tea (*Camellia sinensis*) leaves. *Food Chem.* **2017**, *230*, 637–648. [CrossRef]
14. Pei, D.; Wu, X.; Liu, Y.; Huo, T.; Di, D.; Guo, M.; Zhao, L.; Wang, B. Different ionic liquid modified hypercrosslinked polystyrene resin for purification of catechins from aqueous solution. *Colloids Surf. A Physicochem. Eng. Asp.* **2016**, *509*, 158–165. [CrossRef]
15. Chen, J.; Xue, W.; Shi, Y.; Liu, W.; Ma, R. MXene/MWCNTs-COOH/MOF-808-based electrochemical sensor for the detection of catechin. *Microchem. J.* **2025**, *215*, 114339. [CrossRef]
16. Wang, Y.; Zhao, Z.; Wang, Y.; Liu, Z.; Chen, L.; Qi, J.; Xie, Y.; Zhao, P.; Fei, J. Ultrafine metal-organic framework @ graphitic carbon with MoS_2-CNTs nanocomposites as carbon-based electrochemical sensor for ultrasensitive detection of catechin in beverages. *Microchim. Acta* **2025**, *192*, 40. [CrossRef] [PubMed]
17. Li, J.; Zhu, D.; Huang, H.; Xie, S.; Xu, J.; Yue, R.; Duan, X. High-efficient electrochemical sensing platform based on MOF-doped Au/PEDOT composites toward simultaneous detection of catechin and sunset yellow in tea beverage. *Electrochim. Acta* **2023**, *462*, 142732. [CrossRef]
18. Yan, X.; Hu, X.; Chen, T.; Zhang, S.; Zhou, M. Adsorptive removal of 1-naphthol from water with Zeolitic imidazolate framework-67. *J. Phys. Chem. Solids* **2017**, *107*, 50–54. [CrossRef]
19. Wang, H.; Cheng, Z.; Zhang, P.; Ye, J.; Ding, L.; Jia, W. Ultra-high adsorption behavior of zeolitic imidazole framework-67 nanoparticles for removing brilliant green dye. *AIP Adv.* **2021**, *11*, 095304. [CrossRef]
20. Duan, C.; Yu, Y.; Hu, H. Recent progress on synthesis of ZIF-67-based materials and their application to heterogeneous catalysis. *Green Energy Environ.* **2022**, *7*, 3–15. [CrossRef]
21. Zhong, G.; Liu, D.; Zhang, J. The application of ZIF-67 and its derivatives: Adsorption, separation, electrochemistry and catalysts. *J. Mater. Chem.* **2018**, *6*, 1887–1899. [CrossRef]
22. Qian, J.; Sun, F.; Qin, L. Hydrothermal synthesis of zeolitic imidazolate framework-67 (ZIF-67) nanocrystals. *Mater. Lett.* **2012**, *82*, 220–223. [CrossRef]
23. Li, P.; Yue, X.; Li, A.; Cui, C.; Wang, L.; Tan, W. Electrospun ZIF-67/PVDF composite membranes for efficient ciprofloxacin removal from wastewater. *RSC Adv.* **2025**, *15*, 11503–11510. [CrossRef] [PubMed]
24. Wang, T.; Yue, X.; Han, L.; Wang, J.; Zhang, Y.; Tang, X.; Wang, S. Synthesis of UiO-66-NH2@ SiO2 with a multistage pore structure for effective adsorption of organic pollutants. *Int. J. Low-Carbon Technol.* **2023**, *18*, 1284–1295. [CrossRef]

25. Habib, N.; Gulbalkan, H.C.; Aydogdu, A.S.; Uzun, A.; Keskin, S. Toward rational design of ionic liquid/Metal-Organic Framework composites for efficient gas separations: Combining molecular modeling, machine learning, and experiments to move beyond trial-and-error. *Coord. Chem. Rev.* **2025**, *539*, 216707. [CrossRef]
26. Lv, D.; Cao, X.; Zhang, N.; Cheng, F. Bifunctional ionic liquid-embedded MOFs for constructing ordered CO_2-affinitive channels in CO_2/N_2 separation membranes. *Chem. Eng. Res. Des.* **2025**, *218*, 896–907. [CrossRef]
27. Dai, X.J.; Chen, Y.T.; Zhang, W.G.; Li, S.-X.; Zhang, W.-R.; Qi, X.-H.; Gong, C.-H.; Wang, P.; He, M.-L.; Yang, Y. Ionic liquid modified MOF-808 for efficient adsorption and stable capture of radioactive iodine. *J. Environ. Manag.* **2025**, *392*, 126731. [CrossRef]
28. Yang, Q.; Zhang, Y.; Han, L.; Sheng, J.; Tian, Y. Ionic liquid-functionalized metal-organic frameworks adsorbents for effective extraction of dibutyl phthalate in edible oil: A new strategy for selectivity and low cost. *Food Chem.* **2025**, *482*, 144182. [CrossRef] [PubMed]
29. Fang, L.; Tian, M.; Row, K.H.; Yan, X.; Xiao, W. Isolation of aristolochic acid I from herbal plant using molecular imprinted polymer composited ionic liquid-based zeolitic imidazolate framework-67. *J. Sep. Sci.* **2019**, *42*, 3047–3053. [CrossRef]
30. Chen, P.; Li, X.M.; Yan, X.M.; Tian, M.L. Solid-phase extraction of aristolochic acid I from natural plant using dual ionic liquid-immobilized ZIF-67 as sorbent. *Separations* **2021**, *8*, 22. [CrossRef]
31. Li, X.; Qiao, R.; Jiu, X.; Tian, M. Solid phase extraction of (+)-catechin from cocoa shell waste using dual ionic liquid@ZIF8 covered silica. *Separations* **2022**, *9*, 441. [CrossRef]
32. Tian, M.; Fang, L.; Yan, X.; Xiao, W.; Row, K.H. Determination of heavy metal ions and organic pollutants in water samples using ionic liquids and ionic liquid-modified sorbents. *J. Anal. Methods Chem.* **2019**, *2019*, 1948965. [CrossRef] [PubMed]
33. Yusoff, A.H.M.; Salimi, M.N.; Gopinath, S.C.B.; Abdullah, M.; Samsudin, E. Catechin adsorption on magnetic hydroxyapatite nanoparticles: A synergistic interaction with calcium ions. *Mater. Chem. Phys.* **2020**, *241*, 122337. [CrossRef]
34. Jabbari, A.; Jabbari, M.; Zare, E.N. Synthesis and evaluation of a novel MOF/polymer nanohybrid for pH-sensitive adsorption of two natural products with similar structure. *Talanta* **2025**, *297*, 128807. [CrossRef]
35. Zhu, Y.; Qi, B.K.; Lv, H.N.; Gao, Y.; Zha, S.-H.; An, R.-Y.; Zhao, Q.-S.; Zhao, B. Preparation of DES lignin-chitosan aerogel and its adsorption performance for dyes, catechin and epicatechin. *Int. J. Biol. Macromol.* **2023**, *247*, 125761. [CrossRef]